Characterization of Phosphatidylinositol, Phosphatidylinositol-4-phosphate, and Phosphatidylinositol-4,5-bisphosphate by Electrospray Ionization Tandem Mass Spectrometry: A Mechanistic Study

Fong-Fu Hsu and John Turk

Mass Spectrometry Resource, Division of Endocrinology, Diabetes, and Metabolism, Department of Medicine, Washington University School of Medicine, St. Louis, Missouri, USA

Structural characterization of phosphatidylinositol (PI), phosphatidylinositol-4-phosphate (PI-4P), and phosphatidylinositol-4,5-bisphosphate (PI-4,5-P_2) by collisionally activated dissociation (CAD) tandem mass spectrometry with electrospray ionization is described. In negative ion mode, the major fragmentation pathways under low energy CAD for PI arise from neutral loss of free fatty acid substituents ($[M - H - R_xCO_2H]^-$) and neutral loss of the corresponding ketenes ($[M - H - R'_xCH{=}C{=}O]^-$), followed by consecutive loss of the inositol head group. The intensities of the ions arising from neutral loss of the *sn*-2 substutient as a free fatty acid ($[M - H - R_2CO_2H]^-$) or as a ketene ($[M - H - R'_2CH{=}C{=}O]^-$) are greater than those of ions reflecting corresponding losses of the *sn*-1 substutient. This is consistent with our recent finding that ions reflecting those losses arise from charge-driven processes that occur preferentially at the *sn*-2 position. These features permit assignment of the position of the fatty acid substituents on the glycerol backbone. Nucleophilic attack of the anionic phosphate onto the C-1 or the C-2 of the glycerol to which the fatty acids attached expels *sn*-1 ($R_1CO_2^-$) or *sn*-2 ($R_2CO_2^-$) carboxylate anion, respectively. This pathway is sterically more favorable at *sn*-2 than at *sn*-1. However, further dissociations of $[M - H - R_xCO_2H - \text{inositol}]^-$, $[M - H - R_xCO_2H]^-$, and $[M - H - R'_xCH{=}C{=}O]^-$ precursor ions also yield $R_xCO_2^-$ ions, whose abundance are affected by the collision energy applied. Therefore, relative intensities of the $R_xCO_2^-$ ions in the spectrum do not reflect their positions on the glycerol backbone and determination of their regiospecificities based on their ion intensities is not reliable. The spectra also contain specific ions at *m/z* 315, 279, 259, 241, and 223, reflecting the inositol head group. The last three ions are also observed in the tandem spectra of the $[M - H]^-$ ions of phosphatidylinositol monophosphate (PI-P) and phosphatidylinositol bisphosphate (PI-P_2), in addition to the ions at *m/z* 321 and 303, reflecting the doubly phosphorylated inositol ions. The PI-P_2 also contains unique ions at *m/z* 401 and 383 that reflect the triply phosphorylated inositol ions. The $[M - H]^-$ ions of PI-P and PI-P_2 undergo fragmentation pathways similar to that of PI upon CAD. However, the doubly charged ($[M - 2H]^{2-}$) molecular ions undergo fragmentation pathways that are typical of the $[M - H]^-$ ions of glycerophosphoethanolamine, which are basic. These results suggest that the further deprotonated gaseous $[M - 2H]^{2-}$ ions of PI-P and PI-P_2 are basic precursors. (J Am Soc Mass Spectrom 2000, 11, 986–999) © 2000 American Society for Mass Spectrometry

Phosphoinositides are phospholipids with an inositol group that are widely distributed in nature and which, in animal tissues, are involved in secretory events and in intercellular signaling. The most commonly occurring classes are phosphatidylinositol (PI) (A) and two more highly phosphorylated molecules, phosphatidylinositol-4-phosphate (PI-4-P) (B) and phosphatidylinositol-4,5-bisphosphate (PI-4,5-P_2) (C) (Figure 1).

The metabolism of inositol lipids is involved in the signal transduction of many hormones, neurotransmitters, and growth factors [1–5]. In the classical pathway, the membrane phospholipid phosphatidylinositol-4,5-bisphosphate is hydrolyzed by phospholipase C enzymes to release the second messengers inositol-1,4,5-trisphosphate and 1,2-diacylglycerol with the former inducing the intracellular Ca^{2+} release and the latter activating the protein kinase C isozymes.

Address reprint requests to Fong-Fu Hsu, Department of Medicine, Box 8127, Washington University School of Medicine, St. Louis, MO 63110. E-mail: fhsu@im.wustl.edu

1044-0305/00/$20.00
PII S1044-0305(00)00172-0

Received May 12, 2000
Revised July 6, 2000
Accepted July 6, 2000

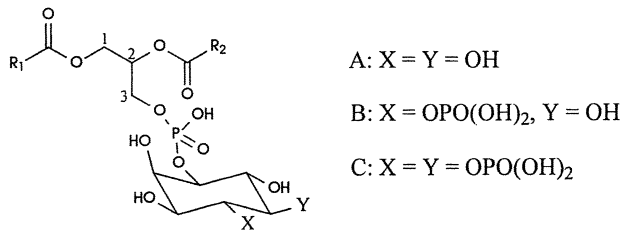

Figure 1. •••

Investigations into the fast atom bombardment (FAB) and electrospray ionization (ESI) mass spectrometric methods of phosphoinositides have focused on PI [6–11], and there are few reports on the tandem mass spectrometry of phosphatidylinositol monophosphate (PI-P) and phosphatidylinositol bisphosphate (PI-P_2) [8]. Both low energy and high energy collisionally activated dissociation (CAD) tandem mass spectra of the $[M - H]^-$ of PI in negative ion mode have been reported [6–11], but the detail mechanism(s) underlying fragmentation under CAD have not yet been described. There is also no report on the structural determination of PI-P and PI-P_2 by tandem mass spectrometry. Recently, we proposed the fragmentation pathways of glycerophosphoethanolamine (GPE) and glycerophosphatidic acid (GPA) under low energy CAD with ESI tandem mass spectrometry [12, 13]. Herein, we extend our studies on phosphoinositides. Results from this study are consistent with our earlier findings that gas-phase basicity of the precursor ions and steric configuration of the molecules are the two determinants that govern the ion formation and lead to the structural characterization. The fragmentation pathways of phosphoinositides under low energy CAD are also proposed.

Experimental

Mass Spectrometry

ESI/MS analyses were performed on a Finnigan TSQ-7000 triple stage quadrupole mass spectrometer equipped with an electrospray ion source and controlled by Finnigan ICIS software operated on a DEC alpha station. Typically, solution of standards were prepared in chloroform/methanol (1/4) at final concentration of 2 pmol/uL, which yields intense deprotonated molecular anions ($[M - H]^-$) and doubly charged anions ($[M - 2H]^{2-}$) by negative ion ESI, depending on the compound. Samples were infused (1 μL/min) into ESI source with a Harvard syringe pump. The electrospray needle and the skimmer were at ground potential and the electrospray chamber and the entrance of the glass capillary were at 4.5 kV. The heated capillary temperature was 250 °C. The precursor ions were selected in the first quadrupole and collided with Ar (2.3 mtorr) in the rf-only second quadrupole, where a potential difference of 40–50 eV for $[M - H]^-$ ions and of 20–25 eV for $[M - 2H]^{2-}$ ions was applied. The precursor ion spectra were obtained in the same manner by selecting the precursor ions in the third quadrupole and mass scanned in the first quadrupole. For CAD tandem mass spectrometry of source-generated fragment ions (source CAD-MS^2), the skimmer voltage was set at 30–35 V to generate abundant fragment ions that were then selected in the first quadrupole, subjected to collision with Ar (2.3 mtorr) in the second quadrupole using a collision energy of 30–35 eV, and analyzed in the third quadrupole.

Materials

Deuterated methanol (CH_3OD) was purchased from Sigma Chemical (St. Louis, MO). All PI, PI-P, and PI-P_2 standards were purchased from either Sigma Chemical or Avanti Polar Lipids (Alasbaster, AL). Solvents and all other chemicals were purchased from Fisher Chemical (Pittsburgh, PA). To perform H–D exchange, standard 16:0/18:2-PI was dissolved in CH_3OD, blown to dryness under a stream of nitrogen, and re-constituted in CH_3OD before ESI analysis.

Results and Discussion

Phosphatidylinositols

In negative ion mode, PI yields abundant $[M - H]^-$ ions by ESI. Following CAD, the $[M - H]^-$ ions yield three major series of fragment ions that reflect neutral loss of free fatty acid ($[M - H - R_xCO_2H]^-$), neutral loss of ketene ($[M - H - R'_xCH{=}C{=}O]^-$), and fatty carboxylate anions ($[R_xCO_2^-]$), where $x = 1,2,$; $R_x = R'_xCH_2$. Ions reflecting an inositol polar head group are also abundant.

Ions Arising from Neutral loss of Free Fatty Acid ($[M - H - R_xCO_2H]^-$) and Neutral Loss of Ketene ($[M - H - R'_xCH{=}C{=}O]^-$)

The CAD tandem mass spectrum of the $[M - H]^-$ ions of 1-hexadecanoyl-2-octadeca-9′,12′-dienoyl *sn*-glycero-3-phosphoinositol (16:0/18:2-PI) at *m/z* 833 (Figure 2A) contains ions at *m/z* 577 and 553, representing neutral losses of the *sn*-1 and *sn*-2 substituents as fatty acids, respectively. Neutral loss of the *sn*-1 or *sn*-2 substituent as a ketene yield ion at *m/z* 595 or 571, respectively (Scheme **1**). The intensities of the ions at *m/z* 553 ($[M - H - R_2CO_2H]^-$) and 571 ($[M - H - R'_2CH{=}C{=}O]^-$), reflecting losses of the *sn*-2 substituents, are respectively more abundant than those of *m/z* 577 ($[M - H - R_1CO_2H]^-$) and *m/z* 595 ($[M - H - R'_1CH{=}C{=}O]^-$), reflecting losses of the substituents at *sn*-1. This is consistent with our recent report that ions deriving from these losses are charge-driven processes that occur more favorably at *sn*-2 [12, 13]. This permits assignment of the positions of the fatty acid moieties on glycerol

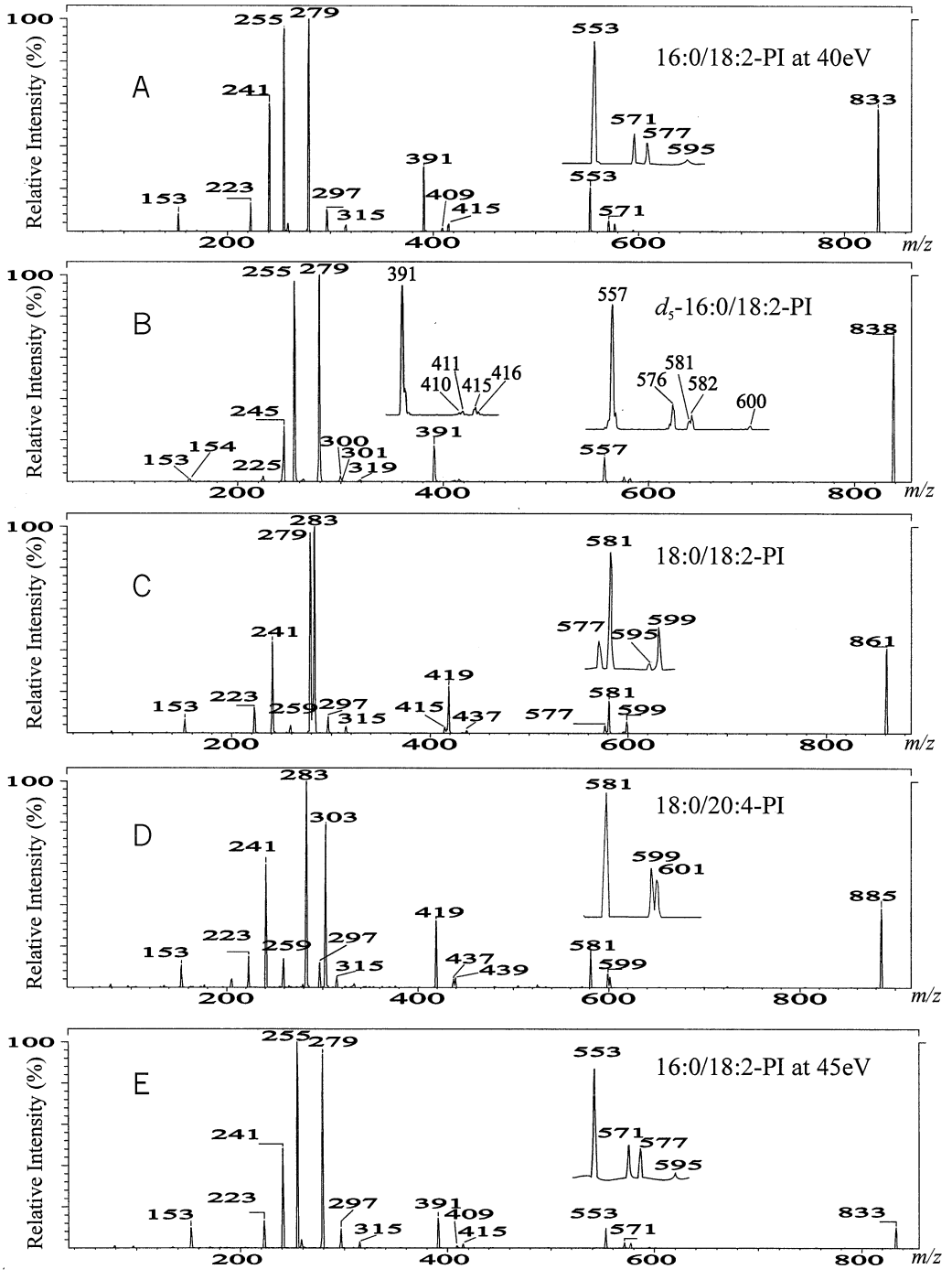

Figure 2. The CAD tandem mass spectra obtained at a collision energy of 40 eV of (**A**) 16:0/18:2-PI, (**B**) d_5-16:0/18:2-PI, where deuteriums were labeled on the 5 hydroxy hydrogen atoms of the inositol by H–D exchange, (**C**) 18:0/18:2-PI, and (**D**) 18:0/20:4-PI. (**E**) Tandem spectrum of 16:0/18:2-PI obtained at 45 eV.

backbone. The intensities of the *m/z* 577 and 553 ions, arising from neutral loss of the acids, are also more abundant than the *m/z* 595 and 571 ions, arising from their ketene loss counterparts (i.e., 577 > 595; 553 > 571). These results are similar to that observed for GPA [13]. This is not surprising since both PI and PA are acidic glycerophospholipids. This is also consistent with our recent finding that neutral loss of acid is a more favorable pathway than loss of ketene for acidic precursor ions such as $[M - H]^-$ ions of GPA [13]. The hydrogen participating in the elimination of the *sn*-2 fatty acid (R_2CO_2H) arises from the exchangeable hydrogen atoms of the molecule. This is evidenced by the tandem spectrum of the *m/z* 838 ion of d_5-16:0/18:2-PI,

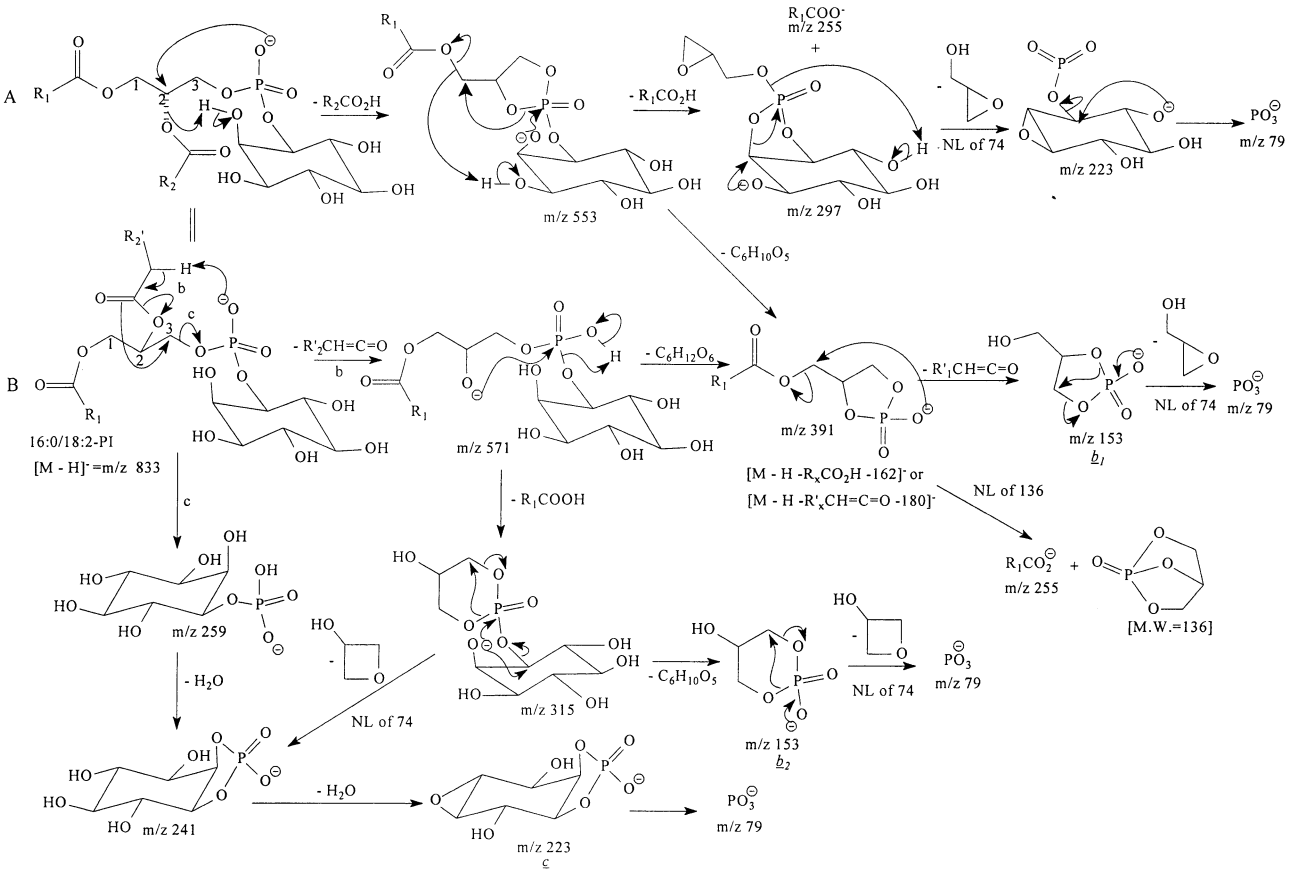

Scheme 1

in which the five hydroxyl hydrogen atoms in inositol have been replaced by deuterium via H–D exchange. The spectrum (Figure 2B) contains the *m/z* 557 ion, reflecting loss of 281 ($C_{17}H_{31}CO_2D$). The participation of the exchangeable hydrogen in the elimination of R_2COOH is further evidenced by the tandem spectra of the same molecule in which H–D exchange is incomplete. For examples, the abundance ratio of *m/z* 556/557 ($[M - H - C_{17}H_{31}CO_2D]/[M - H - C_{17}H_{31}CO_2H]$) is 4/1 for d_4-16:0/18:2-PI (*m/z* 837), of *m/z* 555/556 for d_3-16:0/18:2-PI (*m/z* 836) is 3/2, of *m/z* 554/555 for d_2-16:0/18:2-PI (*m/z* 835) is 2/3, of *m/z* 553/554 for d_1-16:0/18:2-PI (*m/z* 834) is 1/4 (data not shown). The exchangeable hydrogen atoms partially participate in the acid loss at *sn*-1 (R_1CO_2H). This is reflected by the presence of ions at *m/z* 582 and 581 with a ratio of 3/2, arising from neutral losses of $C_{15}H_{31}CO_2H$ and $C_{15}H_{31}CO_2D$, respectively (Figure 2B). Thus, loss of the *sn*-2 fatty acid most likely is a charge-driven process that involves the participation of an acidic hydrogen, whereas loss of *sn*-1 fatty acid may be both a charge-driven and a charge-remote processes. The charge-remote process may involve the participation of the methane hydrogen at C-2 for the loss [12].

Further loss of the inositol head group (loss of 180) from the $[M - H - R'_xCH=C=O]^-$ ions at *m/z* 595 and 571, respectively yields ions at *m/z* 415 and 391, followed by further dissociation to form ions at *m/z* 279 and 255, respectively, via neutral loss of 136 [13] (Scheme **1**). The *m/z* 415 and 391 ions can also arise from loss of *m/z* 162 ([inositol − H_2O]) from the *m/z* 577 and the 553 ions, respectively. The respective expulsion of palmitic acid (R_1CO_2H) and palmitoyl ketene ($R'_1CH=C=O$) from *m/z* 553 yields ions at *m/z* 297 and 315, which are characteristic of PI. The latter two ions can also arise from the respective loss of linoleic acid (R_2CO_2H) and linoleoyl ketene ($R'_2CH=C=O$) from *m/z* 577, a $[M - H - R_1CO_2H]^-$ ion. The *m/z* 595 ($[M - H - R_1CH=C=O]^-$) and 571 ($[M - H - R_2CH=C=O]^-$) ions mainly undergo further loss of linoleic and palmitic acids, respectively, to give *m/z* 315. This is consistent with the idea that the $[M - H - R'_xCH=C=O]^-$ are acidic (or become more acidic) ions, which consecutively undergo an acid loss in preference to a ketene loss [12, 13]. The $[M - H - R_xCO_2H]^-$ precursors also undergo another acid loss to yield the *m/z* 297 ($[M - H - R_1CO_2H - R_2CO_2H]^-$) ion, which is more abundant than the *m/z* 315 ($[M - H - R_1CO_2H - R_2CH=C=O]^- + [M - H - R_2CO_2H - R_1CH=C=O]^-$) ion, arising from an additional ketene loss. This may be due to the fact that the $[M - H - R_xCO_2H]^-$ ions may remain acidic due to the multiple hydroxy groups in inositol (five exchangeable hydrogen atoms), which are responsible for the second acid loss. This assumption is

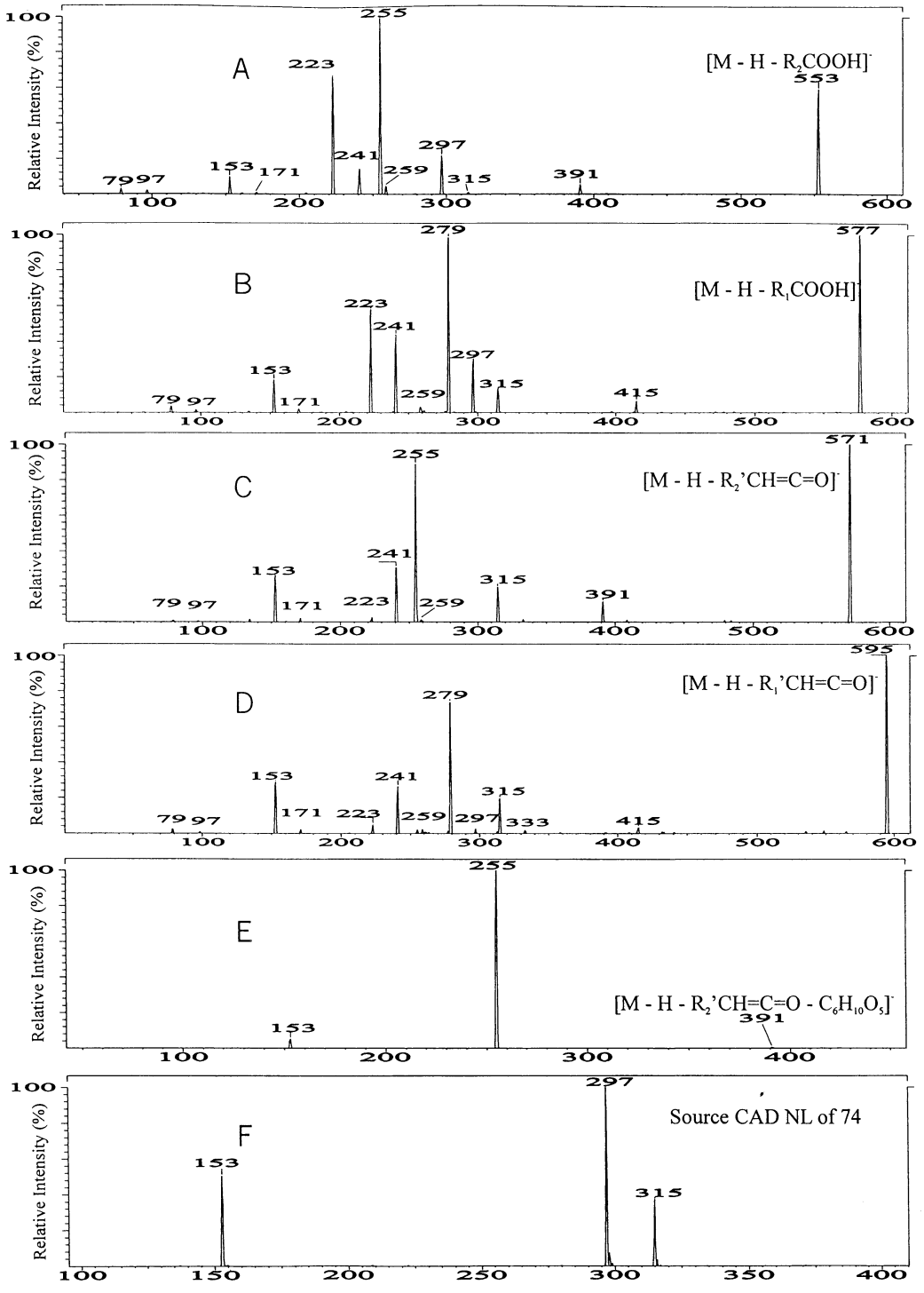

Figure 3. The source CAD tandem mass spectra of (**A**) *m/z* 553 ($[M - H - R_2'COOH]^-$), (**B**) *m/z* 577 ($[M - H - R_1'COOH]^-$), (**C**) *m/z* 571 ($[M - H - R_2'CH{=}C{=}O]^-$), (**D**) *m/z* 595 ($[M - H - R_1'CH{=}C{=}O]^-$), (**E**) *m/z* 391 ($[M - H - R_2'CH{=}C{=}O$ − inositol$]^-$), and (**F**) CNL of 74. The ions were generated by skimmer CAD of 16:0/18:2-PI, and selected in Q1 (A–E), collided in rf-only Q2, and mass analyzed in Q3. Spectrum F was obtained by linked scanning Q1 and Q3 with a constant neutral loss of 74.

based on the observation of *m/z* 300, which represents a $[M - H - R_1CO_2D - R_2CO_2D]^-$ ion (loss of 257 and 281) arising from d_5-16:0/18:2-PI at *m/z* 838 (Figure 2B). The above pathways are supported by source CAD-MS^2 spectra (Figure 3) of the ions at *m/z* 553 (Panel A), 577 (Panel B), 571 (Panel C), 595 (Panel D), 391 (Panel E), and 415 (not shown), arising from 16:0/18:2-PI. The *m/z* 299 ion, which is observed by high-energy

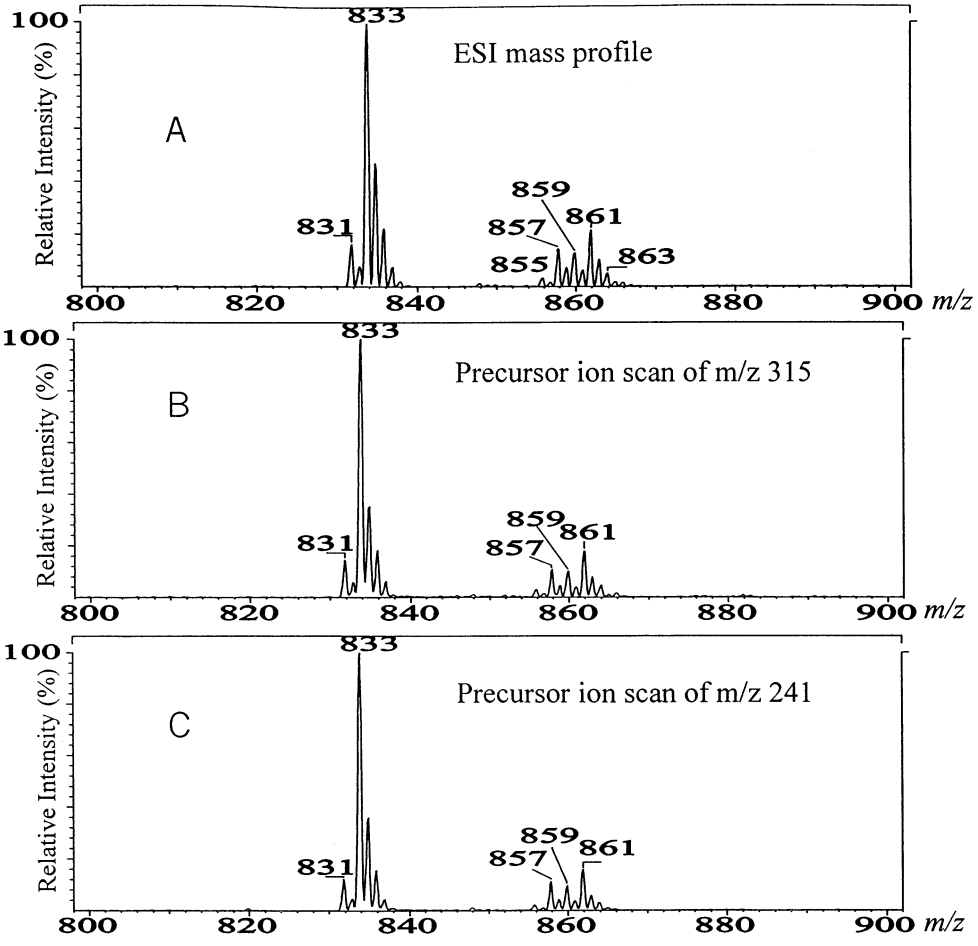

Figure 4. (**A**) The ESI/MS $[M - H]^-$ ion profile of a PI mixture isolated from soybean. The ion current profiles of the same mixture obtained by precursor ion scan of *m/z* 315 (Panel **B**), and of *m/z* 241 (Panel **C**) are identical to the $[M - H]^-$ ion profile (Panel **A**), demonstrating the utility of such scans in the identification of PI class in a mixture.

CAD, is not present [8]. This may be attributed to the fact that formation of the *m/z* 299 ion is a charge-remote process that involves homolytic cleavages of the C–O bond between the carboxylates and C-1 or C-2 of the glycerol to form an isopropenyl inositol phosphate anion ($[CH_2{=}CHCH_2OPO_3C_6H_{11}O_5]^-$) [6, 8]. This CRF pathway is a high-energy process, which may not occur under low-energy CAD.

Several other specific ions reflecting inositol polar head group were observed at *m/z* 259, 241, and 223, in addition to ions at *m/z* 315 and 297 as described earlier. Therefore, precursor ion scanning of these ions can be utilized to identify PI species in mixtures. This is confirmed by the precursor ion spectra (Figure 4) of *m/z* 315 (Panel B), 297 (not shown), 241 (Panel C), 259, and 223 (not shown) of a PI mixture isolated from soybean. The spectra comprise ion profiles identical to the ESI/MS ion profile (Panel A). The structures of the *m/z* 259 and the *m/z* 241 ions were first proposed by Sherman et. al [8]. The major pathways for the formation of ions at *m/z* 259 and 223 arise from decompositions of the *m/z* 315 and the *m/z* 297 ions by elimination of 74 as a oxiranylmethyl or a oxetanyl alcohol ($C_3H_6O_3$) that arises from the glycerol backbone (Scheme **1**). This is supported by the neutral loss scan of 74 (Figure 3F), which gives the above ions, and *m/z* 153, representing a cyclic phosphodiester derivative of glycerol (Scheme **1B**, b_1 and b_2 ion). The *m/z* 223 ion (Scheme **1B**, *c* ion) can also arise from a H_2O loss from *m/z* 241. This is supported by source CAD tandem spectrum of *m/z* 241, which yields ions at *m/z* 223, 97, and 79 (data not shown). The elimination of H_2O may involve the participation of two exchangeable hydrogen atoms of the precursor ion. This is evidenced by the *m/z* 245 and 225 ions observed for d_5-16:0/18:2-PI (Figure 2B), in which the *m/z* 225 ion arises from *m/z* 245 by loss of D_2O. The origin of the above ions and their fragmentation pathways are further supported by the CAD tandem spectra of d_5-16:0/18:2-PI (Figure 2B), 18:0/18:2-PI (*m/z* 861, Figure 2C), 18:0/20:4-PI (*m/z* 885, Figure 2D) and of 16:0/20:4-PI (*m/z* 857, Figure 2E), which contain ions analogous to those described in Figure 2A.

The Carboxylate Anions ([$R_xCO_2^-$])

At collision energies of 40 eV (Figure 2A), the tandem spectrum of the $[M - H]^-$ ion of 16:0/18:2-PI contains the two most prominent ions at *m/z* 255 and 279, corresponding to a 16:0 and an 18:2 carboxylate anion, respectively. The latter ion is slightly more abundant than the former, but the abundance of the *m/z* 255 ion becomes slightly more abundant than that of *m/z* 279 at collision energies of 45 eV (Figure 2E). A series of studies in which collision energies were varied from 20 to 55 eV indicate that the abundance of the $R_xCO_2^-$ ions increases as the collision energy increases. As recently reported, three pathways lead to the formation of the $R_xCO_2^-$ ions [12, 13]. The predominant pathway arises from the nucleophilic attack of the phosphate anionic charge site to expel the *sn*-1 or *sn*-2 substituents as $R_1CO_2^-$ or $R_2CO_2^-$ ions, respectively. This pathway is a charge-driven process, which is sterically more favorable at *sn*-2 than at *sn*-1, and results in an abundance of $R_2CO_2^- > R_1CO_2^-$. The carboxylate anions can also arise from further decomposition of $[M - H - R'_xCH{=}C{=}O - \text{inositol}]^-$ {same *m/z* value as $[M - H - R_xCO_2H - (\text{inositol} - H_2O)]^-$}, $[M - H - R_xCO_2H]^-$, and of $[M - H - R'_xCH{=}C{=}O]^-$ precursor ions. These latter processes prevail as the collision energy increases. As also noted earlier, the gaseous $[M - H]^-$ ions of PIs are acidic precursors, which form the $[M - H - R_xCO_2H]^-$ ions more readily than the $[M - H - R'_xCH{=}C{=}O]^-$ ions. The $[M - H - R_2CO_2H]^-$ and the $[M - H - R'_2CH{=}C{=}O]^-$ ions are also more abundant than the respective $[M - H - R_1CO_2H]^-$ and $[M - H - R'_1CH{=}C{=}O]^-$ counterpart ions, because the former two ions have been preferentially formed. The subsequent elimination of 162 ([inositol − H_2O]) from $[M - H - R_xCO_2H]^-$ results in $[M - H - R_xCO_2H - 162]^-$, which are equivalent to the $[M - H - R_xCOOH]^-$ ions observed in the CAD tandem spectra of GPA. Therefore, the $[M - H - R_xCO_2H - 162]^-$ ions of PI can dissociate to $R_xCO_2^-$ ions by the neutral loss of 136 via the same mechanism as that of GPA [13] (Scheme **1B**, route b). The abundance of *m/z* 255 > *m/z* 279 observed for 16:0/18:2-PI at collision energies of ≥45 eV is mainly attributable to the greater abundance of the *m/z* 553 ($M - H - R_2COOH$) and the 391 ($M - H - R_2COOH$ − inositol) ions, which have been favorably formed, followed by further decomposition to yield *m/z* 255, which supersedes the *m/z* 279 ion arising from the subsequent dissociation of the *m/z* 577 ($M - H - R_1COOH$) and 415 ($M - H - R_1COOH - 162$) ions, which are less abundant. Within the range of the collision energies utilized for the tandem spectra analysis for PI, the carboxylate anions also undergo various degrees of fragmentation after they were formed. The degree of fragmentation depends on the unsaturation of the molecules. Our results indicate that polyunsaturated fatty anions such as 4,7,10,13,16,19-docosahexenoate (4,7,10,13,16,19–22:6) anion at *m/z* 327 readily undergoes fragmentation to give *m/z* 283 by loss of CO_2 and only a 10% (Σ%) fraction of the $R_xCO_2^-$ molecular species survives at collision energies of 35 eV. The arachidonate anion at *m/z* 303 also decomposes to *m/z* 259 ion by the same loss, and only a fraction of 20% (Σ%) of the *m/z* 303 ion survives. In contrast, saturated carboxylate anions like the stearate anion (18:0) at *m/z* 283 undergo little dissociation at the same collision energy (99% retains). Thus, the intensities of the carboxylate anions observed for PI are altered by collision energy. Consequentially, assignment of the positions of the fatty acid substituents in the glycerol backbone is unreliable, if only the relative intensities of carboxylate anions are compared.

Phosphatidylinositol-4-phosphate (PI-4-P) and Phosphatidylinositol-3-phosphate (PI-3-P)

The ESI mass spectra of phosphatidylinositol-4-phosphates (PI-4-P) comprise both a $[M - H]^-$ and a prominent doubly charged anion ($[M - 2H]^{2-}$). Upon CAD, both the $[M - H]^-$ and the $[M - 2H]^{2-}$ ions yield informative fragment ions that identify the structure of the molecule. At collision energies of 20 eV, the $[M - 2H]^{2-}$ ion of 1-octadecanoyl-2-eicosa-5′,8′,11′,14′-tetraenoyl *sn*-glycero-3-phosphatidylinositol-4-phosphate (18:0/20:4-PI-4-P) (*m/z* 482.4, Figure 5A) yields the *m/z* 885 ion by loss of PO_3^-. The nucleophilic attack of the phosphate anionic charge site of the precursors on the C-2 expels the $R_2CO_2^-$ ion and results in the formation of the *m/z* 661 ($[M - 2H]^{2-} - R_2CO_2^-$) (482 × 2 − 303) and the *m/z* 303 ($R_2CO_2^-$) ions, simultaneously (Scheme **2A**). The phosphate anionic site also attacks the C-1 to expel the $R_1CO_2^-$ ion, leading to the formation of the *m/z* 681 ($[M - 2H]^{2-} - R_1CO_2^-$) (482 × 2 − 283) and *m/z* 283 ($R_1CO_2^-$) ions. The intensity of the *m/z* 661 ion is more abundant than the *m/z* 681 ion, and the intensity of the *m/z* 303 ($R_2CO_2^-$) ion is also more abundant than the *m/z* 283 ($R_1CO_2^-$) ion. This is consistent with the notion that charge-driven fragmentation (CDF) processes are sterically more favorable at *sn*-2 over *sn*-1 [12, 13]. Ions corresponding to neutral loss of fatty acids are not observed. The above results suggest that the $[M - 2H]^{2-}$ ion of 18:0/20:4-PI-4-P is a basic precursor ion, in which the anion charge site attacks the C-1 or C-2 of the glycerol to form $R_xCO_2^-$ and $[M - 2H]^{2-} - R_xCO_2^-$ ions, simultaneously. The anionic ion also attacks the α-hydrogen of the fatty acid to eliminate a ketene. This latter process is evidenced by the observation of the *m/z* 339 ($[M - 2H - R_2CH{=}C{=}O]^{2-}$) (482 − 286/2) ion, a doubly charged fragment ion that arises from neutral loss of the *sn*-2 substituent (20:4) as a ketene (Scheme **2B**, route a). An analogous ion arising from the corresponding loss of the *sn*-1 substituent (i.e., the *m/z* 349 ion) is not observed. This is consistent with the idea that CDF is sterically preferred at *sn*-2 over *sn*-1. Therefore, the identities of the fatty acids and their regiospecificity can be easily assigned. The spectrum also contains the *m/z* 395 ion (339 × 2 − 283), which arises from expul-

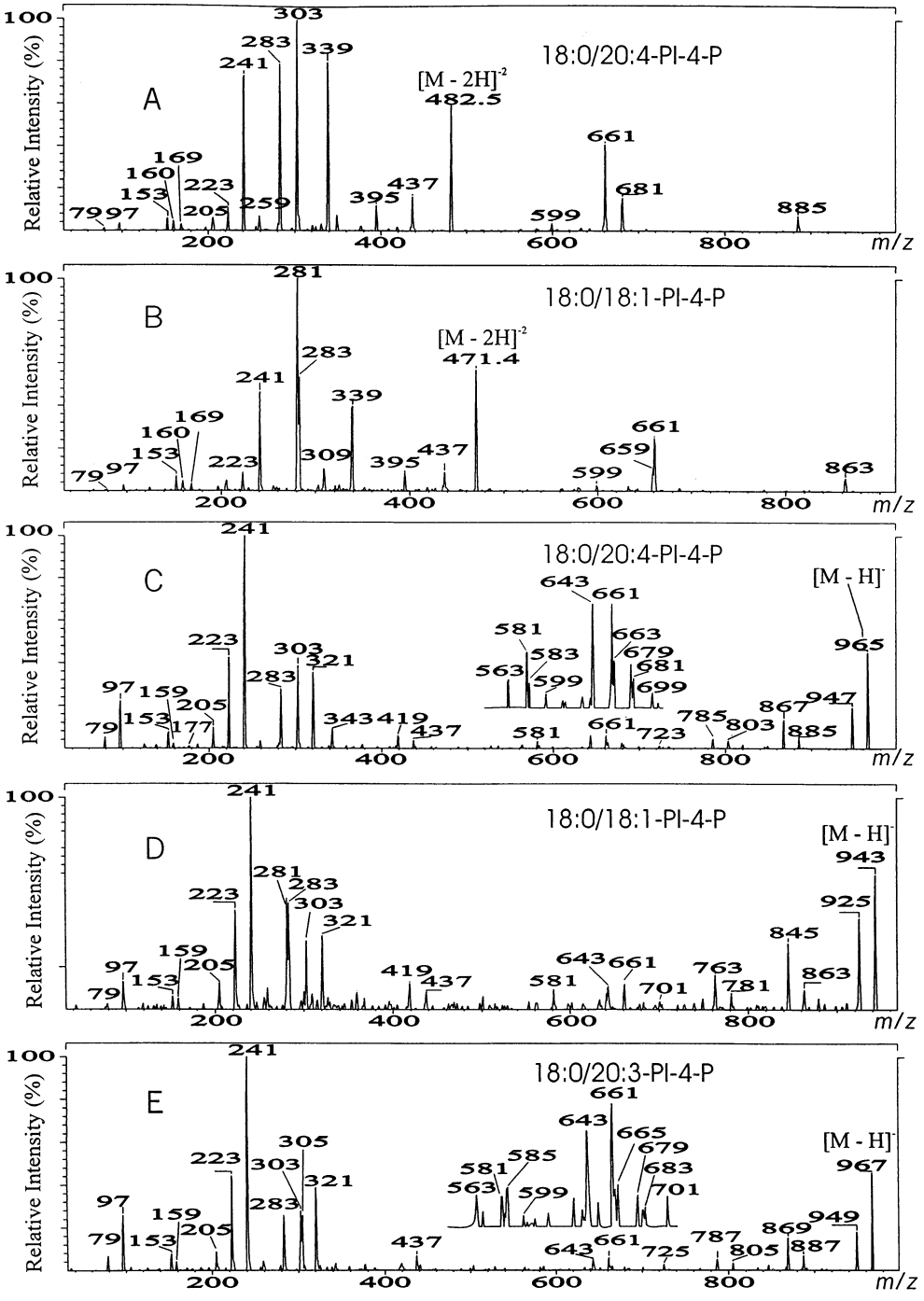

Figure 5. The tandem mass spectra of the $[M - 2H]^{2-}$ ions of (**A**) 18:0/20:4-PI-4-P (*m/z* 482.5), (**B**) 18:0/18:1-PI-4-P (*m/z* 471.4), and the $[M - H]^{-}$ ions of (**C**) 18:0/20:4-PI-4-P (*m/z* 965), (**D**) 18:0/18:1-PI-4-P (*m/z* 943), and (**E**) 18:0/20:3-PI-4-P (*m/z* 967).

sion of the 18:0 carboxylate anion (*m/z* 283) at *sn*-1 from the *m/z* 339 ion (Scheme **2B**, route a_1'). The *m/z* 339 ion also yields the *m/z* 599 ion (339 × 2 − 79), by loss of PO_3^- (Scheme **2B**, route a_3'), and the *m/z* 241 ion (339 × 2 − 437), by loss of 437 (Scheme **2B**, route a_2'). The *m/z* 241 ion can also arise from *m/z* 395 by neutral loss of 154 (Scheme **2B**, route a_{1b}''). This latter process also results in the formation of the *m/z* 153 ion by NL of 242 (Scheme **2B**, a_{1a}''). The above fragmentation pathways and the proposed configuration of the ions are further supported by the source-CAD tandem spectra of the *m/z* 339 and the *m/z* 395 ions (data not shown) and are consistent with the tandem spectrum of the $[M - 2H]^{2-}$ ion at *m/z* 471.4 arising from 18:0/18:1-PI-4-P (Figure 5B).

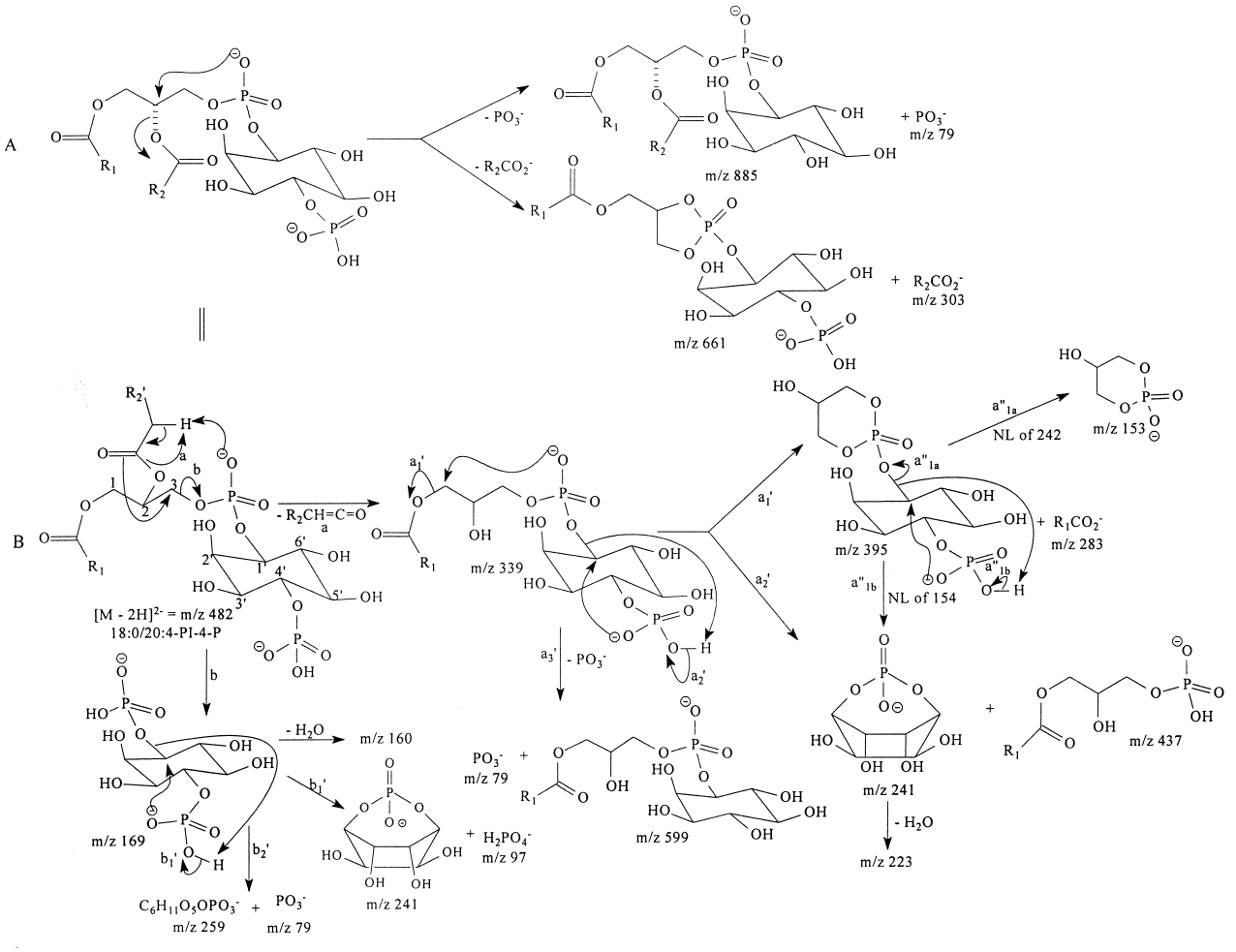

Scheme 2

The additional phosphate in inositol head group is indicated by the observation of the ions at *m/z* 169 and 160, representing a doubly charged inositol bisphosphate ($[C_6H_{10}O_4(OPO_3H)_2]^{2-}$) and a doubly charged dehydrated inositol bisphosphate ($[C_6H_{10}O_4(OPO_3H)_2 - H_2O]^{2-}$) anion, respectively (Scheme **2B**, route b). The *m/z* 169 ion may, again, undergo further dissociation to yield singly charged ion species at *m/z* 241 and 97 ($H_2PO_4^-$) (Scheme **2B**, route b_1') or at *m/z* 259 and 79 (PO_3^-) (Scheme **2B**, route b_2'), simultaneously. The *m/z* 169 and 160 ions plus ions at *m/z* 259, 241, and 223, which reflect the polar head group of the molecule, permit identification of PI-Ps and classification of the phosphorylation state of the inositol head group.

The tandem spectra arising from the $[M - H]^-$ ions of PIPs also contain abundant fragment ions, which are informative for structure determination. This is exemplified by the CAD tandem spectrum of 18:0/20:4-PI-4-P at *m/z* 965 as shown in Figure 5C. The *m/z* 661 and the *m/z* 679 ions correspond to the $[M - H - R_2COOH]^-$ and $[M - H - R_2CH{=}C{=}O]^-$ ions, respectively (Scheme **3A**, routes a and b). The former ion is five times more abundant than the latter, suggesting that the gaseous $[M - H]^-$ ions of the 18:0/20:4-PI-4-P are acidic precursors, which would preferentially undergo acid to ketene loss. This is supported by the observation of the abundance of *m/z* 681 ($[M - H - R_1COOH]^-$) > *m/z* 699 ($[M - H - R_1CH{=}C{=}O]^-$). The intensities of the *m/z* 679 and the *m/z* 661 ions are also more abundant than their respective counterpart ions at *m/z* 681 and 699, consistent with the notion that neutral loss of ketene or acid at *sn*-2 is sterically more favorable. Ions at *m/z* 785 ($[M - H - \text{inositol}]^-$) and 803 ($[M - H - (\text{inositol} - H_2O)]^-$) correspond to loss of inositol and [inositol − H_2O] moieties, respectively. The formation of the former ion may arise from the attack of the anionic charge site of the C4′-phosphate onto the phosphorus of the head group phosphate to eliminate the inositol (Scheme **3B**, route f). The similar attack of the anionic charge site to expel a $C_6H_{10}O_5$ molecule leads to the formation of the *m/z* 803 ion (Scheme **3B,** route g). These pathways are in accord with the presence of ions at the *m/z* 159 and 177, corresponding to a $(PO_3)(HPO_3)^-$ and a $(H_2PO_3)(OPO_3H)^-$ ion, respectively. Several ions arising from water loss were observed at *m/z* 947 (965 −

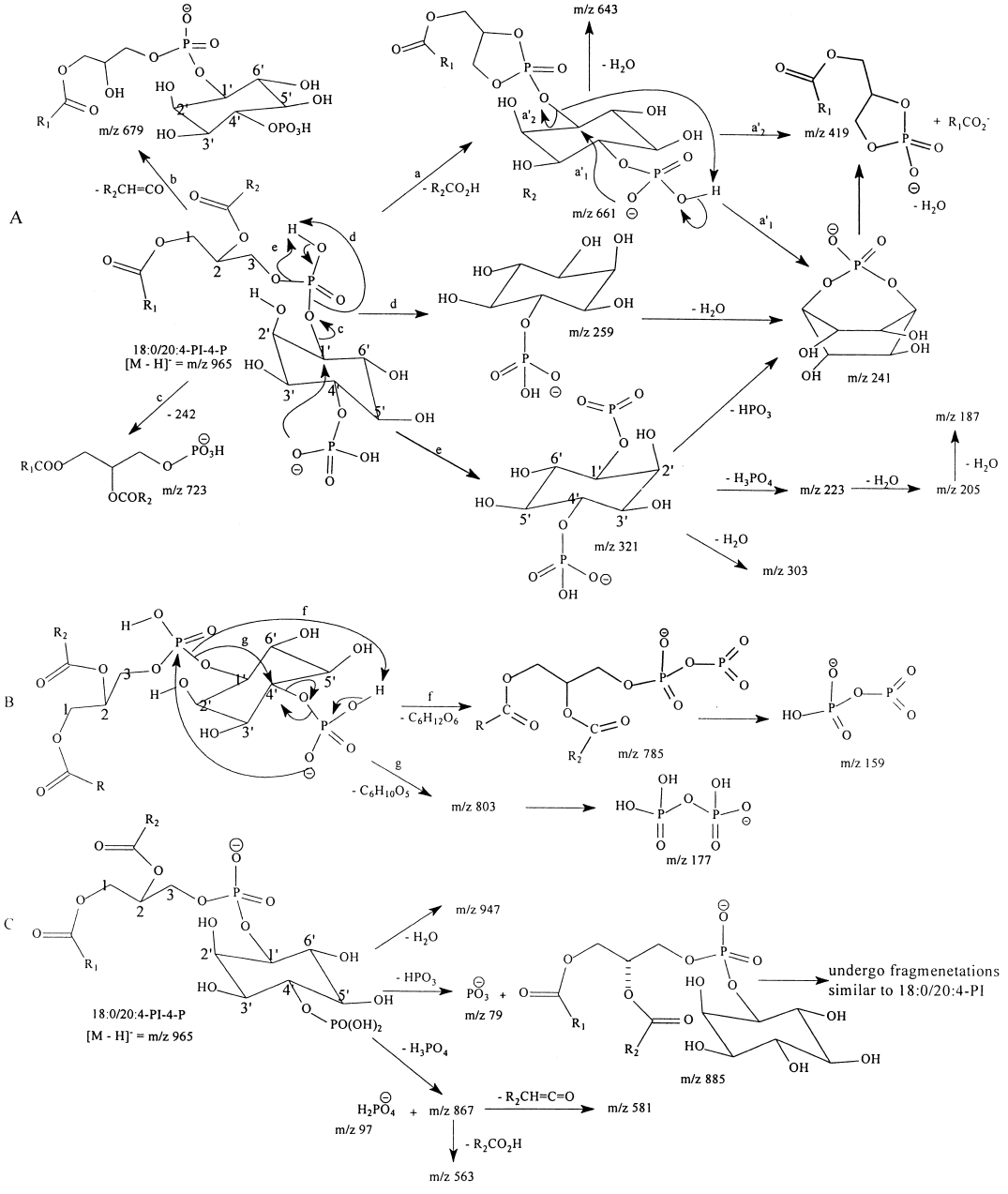

Scheme 3

H_2O), 663 (681 − H_2O), and 643 (661 − H_2O). The spectrum also contains ions at *m/z* 885 and 867, arising from loss of HPO_3 and H_3PO_4, respectively (Scheme **3C**). The former ion undergoes fragmentation (data not shown) identical to that of the $[M - H]^-$ ion of 18:0/20:4-PI (Figure 2D).

In addition to the ions at *m/z* 259, 241, 223, 153, 97, and 79 that are also observed for PI, the spectrum also contains the *m/z* 321 ion (Scheme **3A**, route e), corresponding to a dehydrated inositol bisphosphate, which gives the *m/z* 303 ion by loss of H_2O. These two ions reflect the additional phosphate substitution of the PI-P head group and were observed in the tandem spectra of the $[M - H]^-$ ions of all the PI-4-P and PI-3-P examined. This feature is demonstrated by the precursor ion scans of *m/z* 321 (Figure 6B), 303 (not shown), and 241 (Figure 6C) ions of a PI-4-P mixture from bovine brain extract, which exhibits a profile similar to the total $[M - H]^-$ ion current profile (Figure 6A). The *m/z* 303 ion can also arise from the 20:4 carboxylate anion at *sn*-2. This is evidenced by the CAD tandem spectrum of the 18:0/20:3-PI-4-P at *m/z* 967 (Figure 5E), which contains ions at *m/z* 303 and 305, with the latter ion corresponding to a 20:3 carboxylate ion. The proposed fragmentation pathways as exemplified by the $[M - H]^-$ ion of 18:0/20:4-PI-4-P (*m/z* 965) are depicted in Scheme **3**.

The tandem spectrum of 18:0/20:4-PI-4-P at *m/z* 965 contains abundant carboxylate anions at *m/z* 303 and

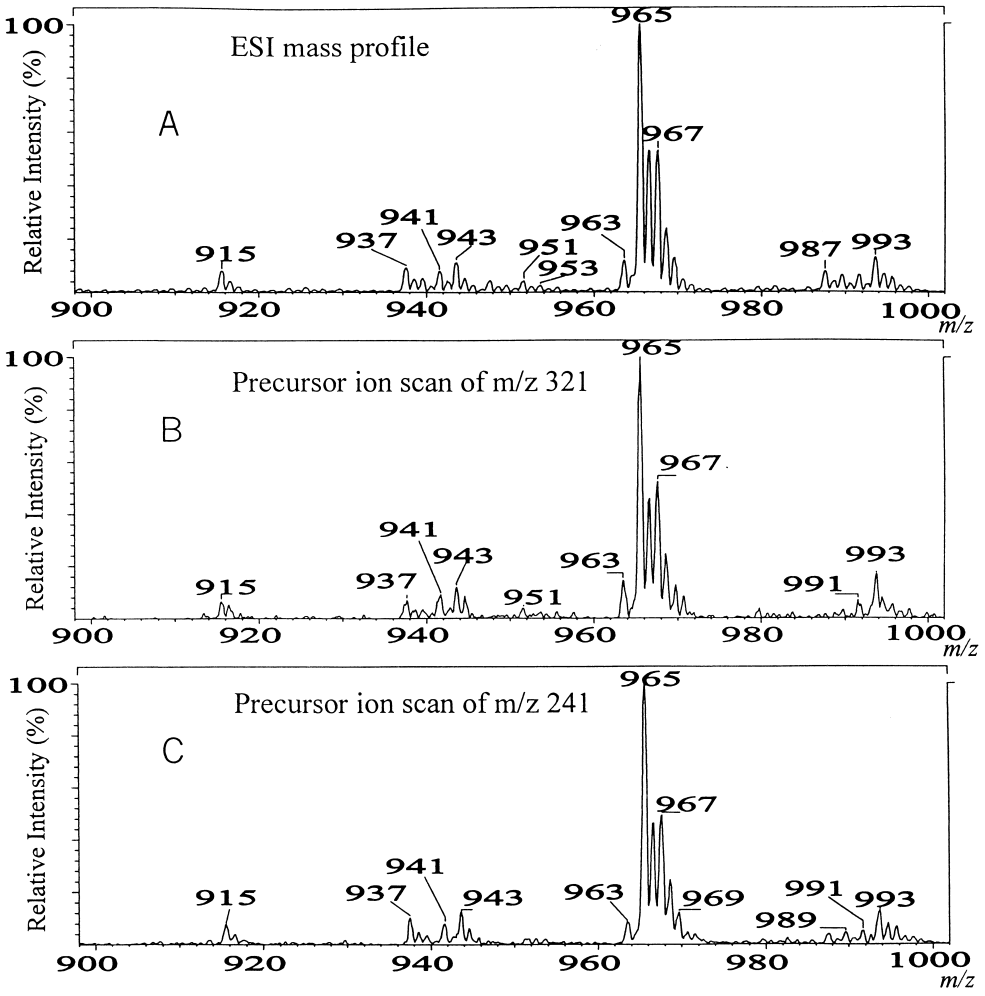

Figure 6. (**A**) The ESI/MS $[M - H]^-$ ion profile of a PI-4-P mixture isolated from bovine brain. The ion current profiles of the same mixture obtained by precursor ion scan of *m/z* 321 (**B**), and of 241 (**C**) are identical to profile (**A**).

283, corresponding to an R_2COO^- and an R_1COO^- ion, respectively. The former ion is more abundant than the latter. However, a nearly equal intensities of the R_2COO^- and R_1COO^- ions were observed for 18:0/18:1-PI-4-P (*m/z* 283 and 281, Figure 5D) and for 18:0/20:3-PI-4-P (*m/z* 283 and 305, Figure 5E), consistent with what has been observed for PIs. This reflects the fact that the *m/z* 321 ion for PI-4-Ps undergoes a H_2O loss to from the *m/z* 303 ion ($[PO_3C_6H_8O_3OPO_3H]^-$), which overlaps with the 20:4 carboxylate anion of *m/z* 303 ($C_{19}H_{31}COO^-$), because the two ions are not resolvable by a quadrupole mass spectrometer. Therefore, pathways leading to the formation of the carboxylate anions for PI-4-Ps may be similar to those for PIs, which are also acidic. The R_2COO^- ion is more abundant than the R_1COO^- ion in the tandem spectra of *m/z* 482.5 (Figure 5A) and 471.4 (Figure 5B), the doubly charged precursor ions for 18:0/20:4-PI-4-P and 18:0/18:1-PI-4-P, respectively. Again, this is consistent with the notion that $[M - 2H]^{2-}$ is a basic precursor ion, which undergoes a GPE-like fragmentation and results in the formation of $R_2COO^- > R_1COO^-$ [12]. The abundance ratio of the R_1COO^-/R_2COO^- (*m/z* 283/281) arising from the *m/z* 943 ($[M - H]^-$) ion of 18:0/18:1-PI-4-P also increases as the collision energy increases (data not shown), consistent with the results observed for GPA [13].

The phosphatidylinositol-3-phosphate (PI-3-P) also yields both a $[M - H]^-$ and a $[M - 2H]^{2-}$ ions by ESI. As exemplified by 16:0/16:0-PI-3-P, the molecule yields a $[M - H]^-$ at *m/z* 889 and a $[M - 2H]^{2-}$ at *m/z* 444.5 (Figure 7A). However, the intensity of the former ion becomes more abundant than the latter, a reversal to that observed for PI-4-P. Both the CAD tandem mass spectra of the *m/z* 444.5 (Figure 7B) and the *m/z* 889 (Figure 7C) ions of 16:0/16:0-PI-3-P are similar to those obtained from PI-4-P. However, the fragment ion representing neutral loss of H_3PO_4 is much more abundant in the tandem spectra arising from the $[M - H]^-$ ion of the latter. This is illustrated by the tandem spectra of 18:0/20:4-PI-4-P at *m/z* 965 (Figure 5C), which yields both the *m/z* 885 and 867 ions; of 18:1/18:0-PI-4-P (Figure 5D), which yields ions at *m/z* 863 and 845; and of

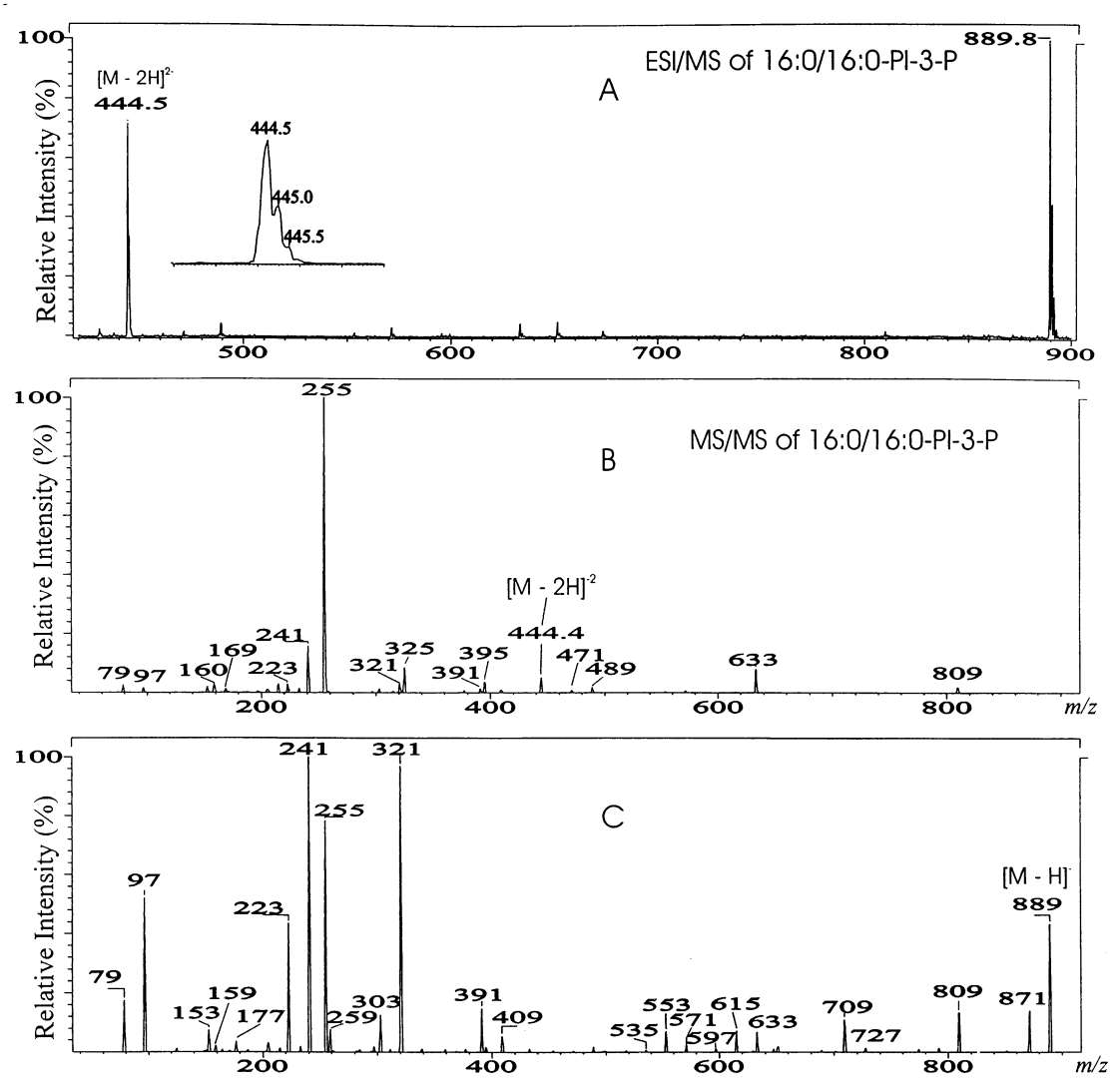

Figure 7. The ESI/MS of 16:0/16:0-PI-3-P (**A**), and its CAD tandem mass spectra obtained from the $[M - 2H]^{2-}$ precursor ions at *m/z* 444.4 (**B**), and from the $[M - H]^{-}$ precursor ions at *m/z* 889 (**C**).

18:0/20:3-PI-4-P (Figure 5E), which yields ions at *m/z* 887 and 869, by losses of HPO_3 and H_3PO_4, respectively. In contrast, the 16:0/16:0-PI-3-P yields the *m/z* 809 ion by loss of HPO_3 and the *m/z* 791 ion reflecting a H_3PO_4 loss is in small abundance. Therefore, loss of H_3PO_4 is a more favorable pathway for PI-4-Ps and this feature permits their distinction from the PI-3-P isomers.

Phosphatidylinositol-4,5-bisphosphate (PI-4,5-P_2) and Phosphatidylinositol-3,4-bisphosphate (PI-3,4-P_2)

By ESI, the 18:0/20:4-PI-4,5-P_2 yields a major $[M - H]^{-}$ ion at *m/z* 1045, and a minor $[M - 2H]^{2-}$ at *m/z* 522.5. A triply charged anion ($[M - 3H]^{3-}$) at *m/z* 347.9 was not observed (data not shown). It appears that the charge state of the ions and their relative intensity do not reflect the number of phosphates attached to the molecule. The tandem spectrum of the *m/z* 1045 ion (Figure 8A) contains abundant fragment ions similar to those arising from 18:0/20:4-PI-4-P. Ions at *m/z* 965, 947, and 929 correspond to losses of HPO_3, H_3PO_4, and ($H_3PO_4 + H_2O$), respectively. The expulsion of one HPO_3, followed by elimination of the inositol or (inositol $- H_2O$) moieties yields the *m/z* 785 ($[M - H - HPO_3 -$ inositol$]^{-}$) or 803 ($[M - H - HPO_3 -$ (inositol $- H_2O$)$]^{-}$) ion, respectively. This pathway comes along with the formation of *m/z* 177 and 159, representing a $(H_2PO_3)(OPO_3H)^{-}$ and a $(PO_3)(HPO_3)^{-}$ ion, respectively, and has been described for PI-P earlier. The combined losses of H_3PO_4 and *m/z* 304 (R_2COOH) lead to the formation of the *m/z* 643 ion, which is more abundant than the *m/z* 663 ion, arising from the combined losses of H_3PO_4 and *m/z* 284 (R_1COOH). This is consistent with the notion that neutral loss of fatty acid at *sn*-2 is sterically more favorable than at *sn*-2, and thus the position of the fatty acid moieties in glycerol backbone can be assigned. The ions reflecting loss of ketenes are not present, consistent with the fact that the

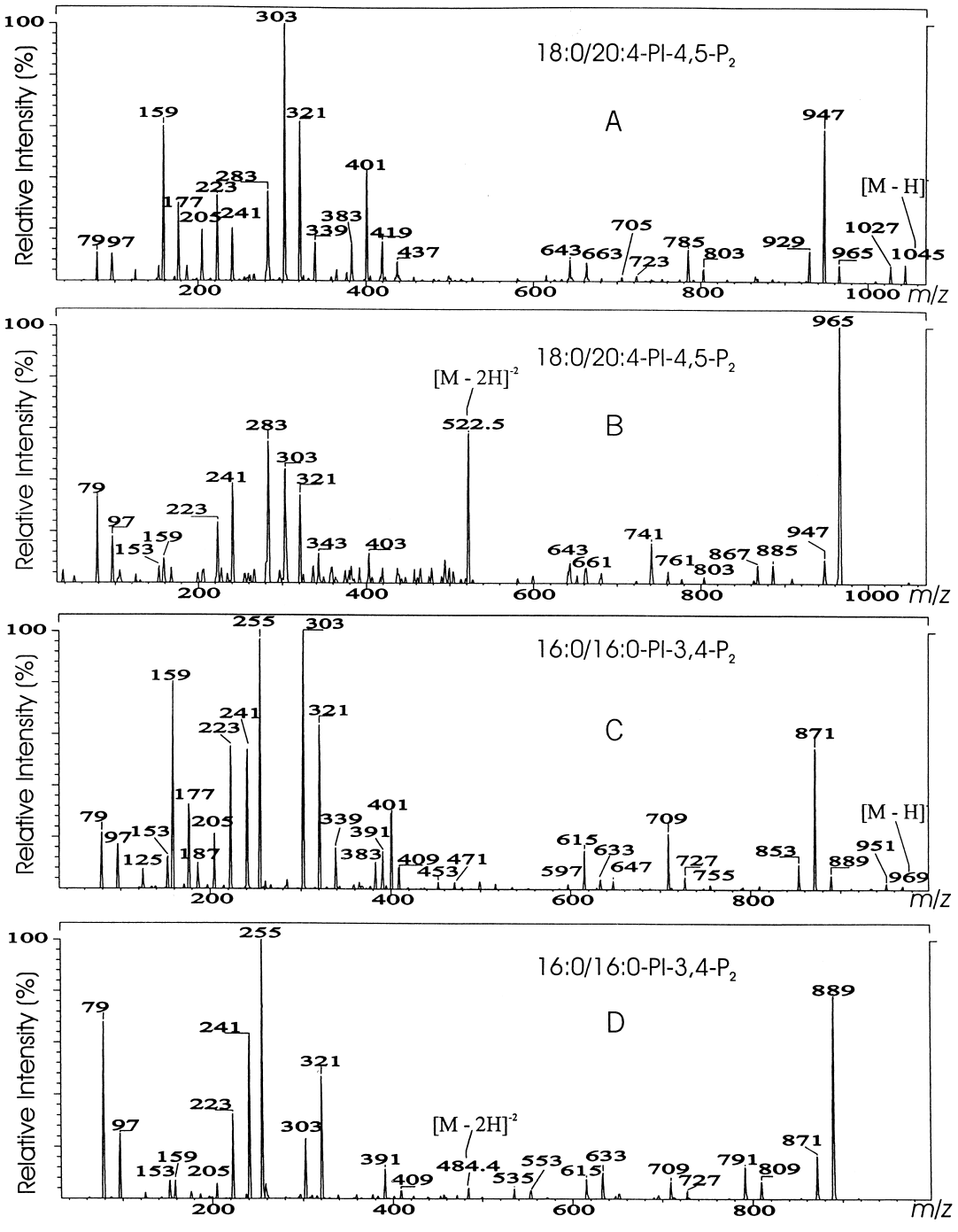

Figure 8. The CAD tandem mass spectra of 18:0/20:4-PI-4,5-P_2 obtained from (**A**) the $[M - H]^-$ precursor ions at *m/z* 1045 and (**B**) from the $[M - 2H]^{2-}$ precursor ions at *m/z* 522.4. The CAD tandem spectra of 16:0/16:0-PI-3,4-P_2 obtained from the $[M - H]^-$ ions at *m/z* 969 and the $[M - 2H]^{2-}$ ions at *m/z* 484.4 are shown in (**C**) and (**D**), respectively.

precursor is an acidic anion, which undergoes a more facile loss of acid rather than a ketene. The common ions observed for PI-4-P and PI-3-P classes, such as *m/z* 321, 303, 241, 223, etc., are abundant. Additionally, a prominent ion at *m/z* 401, reflecting a dehydrated inositol trisphosphate anion as a singly charged species is also present. This is consistent with the earlier finding that PI-Ps yield a *m/z* 321 ion, representing a dehydrated inositol bisphosphate anion (Scheme **3**). The *m/z* 401 and 321 ions also yield *m/z* 383 and 303 ions, respectively, by loss of H_2O. These ions permit identification of the phosphorylation state of the head group and assignment of the parent species as a PIP_2 isomer.

The $[M - H]^-$ ion of 18:0/20:4-PI-4,5-P_2 (*m/z* 522.4, Figure 8B) undergoes fragmentations similar to the $[M - 2H]^{2-}$ ion of PI-4-P as described earlier. Again,

the preferential loss of $R_2CO_2^-$ over $R_1CO_2^-$ leads to the formation of *m/z* 741 (522 × 2 − 303) > *m/z* 761 (522 × 2 − 283). This feature of the tandem spectrum permits assignment of fatty acyl moieties in glycerol backbone. However, doubly charged fragment ions at *m/z* 379, reflecting a ketene loss ($[M - 2H - R_2CH{=}C{=}O]^{2-}$), and ions at *m/z* 169 and 160, representing an inositol bisphosphate ($[C_6H_{10}O_4(OPO_3H)_2]^{2-}$) and a dehydrated inositol bisphosphate ($[C_6H_{10}O_4(OPO_3H)_2 - H_2O]^{2-}$) anions, respectively, are absent. This may be attributable to the fact that the gaseous $[M - 2H]^{2-}$ ions of 18:0/20:4-PI-4,5-P_2 are more acidic than 18:0/20:4-PI-4-P due to the attachment of an additional phosphate moiety, which deters the nucleophilic attack of the anionic charge site on C-1 or C-2 of the glycerol to form a carboxylate anion, as well as on the α-hydrogen of the carboxylate to expel a ketene. Indeed, ions at *m/z* 303 and 283 ions, representing an R_2COO^- and an R_1COO^- ion, respectively, are also less prominent than that observed for 18:0/20:4-PI-4-P (Figure 5A). It is interesting to note that the *m/z* 370 ($[M - 2H - R_2COOH]^{-2}$) ion, arising from an acid loss is also absent.

The ESI spectrum of the 16:0/16:0-PI-3,4-P_2 also comprises a major $[M - H]^-$ ion at *m/z* 969, and a $[M - 2H]^{2-}$ ion at *m/z* 484.4, with the former two times more abundant than the latter (data not shown). Fragment ions arising from the $[M - H]^-$ ion at *m/z* 969 (Figure 8C) are similar to those arising from PI-4,5-P_2 and thus, isomer differentiation between these two subclasses by their tandem mass spectra may not be possible. The tandem spectrum of the $[M - 2H]^{2-}$ precursor ions of 16:0/16:0-PI-3,4-P_2 (*m/z* 484.4, Figure 8D) contains ions analogous to those arising from 18:0/20:4-PI-4,5-P_2 (*m/z* 522.4, Figure 8B). Again, the ion abundance (Σ%) of the R_xCOO^- ion (R_1COO^-=R_2COO^-) at *m/z* 255 (Figure 8D) is less than the same ion observed in 16:0/16:0-PI-3-P (Figure 7B) and the *m/z* 365 (484 − 238/2) ion, which represents a $[M - 2H - R_2CH{=}C{=}O]^{2-}$ ion, is not present, consistent with the results observed for PI-4,5-P_2.

Conclusions

The fragmentation pathways of PI, PI-P, and PI-P_2 under low energy CAD are governed by their steric configuration and their gas-phase acid-base properties, consistent with our recent report for GPA and GPE. CAD tandem mass spectrometry with electrospray ionization is proven to be a powerful tool for structural characterization of PI, PI-P, and PI-P_2.

Acknowledgments

This research was supported by US Public Health Service Grants P41-RR-00954, R37-DK-34388, P60-DK-20579, and P01-HL-57-278 and a grant (No. 996003) from the Juvenile Diabetes Foundation.

References

1. Berridge, M. J. Cell signalling. A tale of two messengers. *Nature* **1993,** *365*, 388–389.
2. Ashcroft, S. J. Intracellular second messengers. *Adv. Exp. Med. Biol.* **1997,** *426*, 73–80.
3. Liscovitch, M.; Cantley, L. C. Lipid second messengers. *Cell* **1994,** *77*, 329–334.
4. Quest, A. F.; Ghosh, S.; Xie, W. Q.; Bell, R. M. DAG second messengers: molecular switches and growth control. *Adv. Exp. Med. Biol.* **1997,** *400A*, 297–303.
5. Strum, J. C.; Ghosh, S.; Bell, R. M. Lipid second messengers. A role in cell growth regulation and cell cycle progression. *Adv. Exp. Med. Biol.* **1997,** *407*, 421–431.
6. Jensen, N. J.; Tomer, K. B.; Gross, M. L. FAB MS/MS for phosphatidylinositol, -glycerol, -ethanolamine and other complex phospholipids. *Lipids* **1987,** *22*, 480–489.
7. Murphy, R. C.; Harrison, K. A. Fast atom bombardment mass spectrometry of phospholipids. *Mass Spectrom. Rev.* **1994,** *13*, 57–75.
8. Sherman, W. R.; Ackermann, K. E.; Bateman, R. H.; Green, B. N.; Lewis, I. Mass-analysed ion kinetic energy spectra and B1E-B2 triple sector mass spectrometric analysis of phosphoinositides by fast atom bombardment. *Biomed. Mass Spectrom.* **1985,** *8*, 409–413.
9. Cronholm, T.; Viestam-Rains, M.; Sjovall, J. Decreased content of arachidonoyl species of phosphatidylinositol phosphates in pancreas of rats fed on an ethanol-containing diet. *Biochem. J.* **1992,** *287*, 925–928.
10. Smith, P. B.; Snyder, A. P.; Harden, C. S. Characterization of bacterial phospholipids by electrospray ionization tandem mass spectrometry. *Anal. Chem.* **1995,** *67*, 1824–1830.
11. Kerwin, J. L.; Tuininga, A. R.; Ericsson, L. H. Identification of molecular species of glycerophospholipids and sphingomyelin using electrospray mass spectrometry. *J. Lipid Res.* **1994,** *35*, 1102–1114.
12. Hsu, F. F.; Turk, J. Charge-remote and charge-driven fragmentation processes in diacyl glycerophosphoethanolamine upon low-energy collisional activation. A mechanistic proposal. *J. Am. Soc. Mass Spectrom.* **2000,** *11*, 892–899.
13. Hsu, F. F.; Turk, J. Charge-driven fragmentation processes in diacyl glycerophosphatidic acids upon low-energy collisional activation. A mechanistic proposal. *J. Am. Soc. Mass Spectrom.* **2000,** *11*, 797–803.